


# Convolutional Neural Networks for Radiologic Images: A Radiologist's Guide

Shelly Soffer, BMedSc • Avi Ben-Cohen, MSc • Orit Shimon, MD • Michal Marianne Amitai, MD • Hayit Greenspan, PhD • Eyal Klang, MD

From the Department of Diagnostic Imaging, Sheba Medical Center, Emek HaEla St 1, Ramat Gan, Israel (S.S., M.M.A., E.K.); Faculty of Engineering, Department of Biomedical Engineering, Medical Image Processing Laboratory, Tel Aviv University, Tel Aviv, Israel (A.B., H.G.); and Sackler School of Medicine, Tel Aviv University, Tel Aviv, Israel (S.S., O.S.). Received March 5, 2018; revision requested April 6; final revision received September 7; accepted September 12. **Address correspondence to E.K.** (e-mail: eyalkla@botmail.com).

Conflicts of interest are listed at the end of this article.

Radiology 2019; 290:590–606 • <https://doi.org/10.1148/radiol.2018180547> • Content code: 

Deep learning has rapidly advanced in various fields within the past few years and has recently gained particular attention in the radiology community. This article provides an introduction to deep learning technology and presents the stages that are entailed in the design process of deep learning radiology research. In addition, the article details the results of a survey of the application of deep learning—specifically, the application of convolutional neural networks—to radiologic imaging that was focused on the following five major system organs: chest, breast, brain, musculoskeletal system, and abdomen and pelvis. The survey of the studies is followed by a discussion about current challenges and future trends and their potential implications for radiology. This article may be used as a guide for radiologists planning research in the field of radiologic image analysis using convolutional neural networks.

©RSNA, 2019

**Online SA-CME** • See [www.rsna.org/learning-center-ry](http://www.rsna.org/learning-center-ry)

#### Learning Objectives:

After reading the article and taking the test, the reader will be able to:

- Describe the fundamental concepts of deep learning and artificial neural networks
- Identify computer vision tasks
- Describe common radiologic applications in deep learning research

#### Accreditation and Designation Statement

The RSNA is accredited by the Accreditation Council for Continuing Medical Education (ACCME) to provide continuing medical education for physicians. The RSNA designates this journal-based SA-CME activity for a maximum of 1.0 AMA PRA Category 1 Credit™. Physicians should claim only the credit commensurate with the extent of their participation in the activity.

#### Disclosure Statement

The ACCME requires that the RSNA, as an accredited provider of CME, obtain signed disclosure statements from the authors, editors, and reviewers for this activity. For this journal-based CME activity, author disclosures are listed at the end of this article.

In the past few decades, developments in medical imaging technology and the increased role of imaging within the diagnostic process have resulted in a rapid expansion of recorded medical visual data, generating a need for novel computational models (1). Several image analysis models were developed, and the latest advancement in this field is a technique called deep learning.

Deep learning is considered by some to be an integral part of the Fourth Industrial Revolution (2). A major breakthrough in the field of deep learning was presented by Lecun and colleagues in 1998 (3), whereby they applied their novel convolutional neural network (CNN), LeNet, to handwritten digit classification. Deep learning-based methods, however, did not receive wide acknowledgment until 2012, in the ImageNet challenge for the classification of more than a million images into 1000 classes. In this competition, Krizhevsky and Hinton (4) successfully developed a CNN named AlexNet that surpassed other competing classic machine learning techniques. Today, CNN is considered to represent the state of the art in image analysis (5,6).

Comprehensive academic research, as well as start-up endeavors, is working on finding deep learning solutions

that can be applicable to the medical world. This is particularly important to the field of radiology, with its visual-based data (6–8).

Several deep learning reviews have been published in the last few years. Some have focused primarily on deep learning methodology (5,9,10). Other reviews, such as the article by Litjens et al on studies published until February of 2017 (6), have presented a comprehensive survey of the literature with an overview of deep learning techniques and applications (6,11–13). Given the sharp surge in the volume of deep learning articles published in medical journals in 2017 that is commensurate with the trend of growing awareness and interest in deep learning within the radiologic community, the time appears optimal for presenting a guide on deep learning for radiologists that includes a general framework of deep learning research and its applications in the field of radiology.

In this review, we aim to provide the radiologist with (a) an introduction to deep learning technology, including relevant terminology; (b) an understanding of the general framework of a radiologic deep learning study; and (c) an overview of the literature on CNN application in radiologic image analysis according to anatomic region.

**This copy is for personal use only. To order printed copies, contact [reprints@rsna.org](mailto:reprints@rsna.org)**

## Abbreviations

AI = artificial intelligence, CNN = convolutional neural network, CONV = convolution, ReLU = rectified linear unit

## Summary

This article is a guide to convolutional neural network technologies and their clinical applications in the analysis of radiologic images.

## Essentials

- The design process of convolutional neural network research includes defining the clinical question, choosing a predefined computer vision task, generating data acquisition and data preprocessing, selecting hardware and software solutions, developing a network architecture, and validating the algorithm performance.
- Current research has applied convolutional neural networks to various organ systems and pathologic disorders, including the following five major anatomic regions: chest, breast, brain, musculoskeletal system, and abdomen and pelvis.

## Overview of Deep Learning Technology

### The Basic Concept of CNNs

CNN algorithms are a subclass in the hierarchic terminology that includes artificial intelligence (AI), machine learning, and deep learning (14). Figure 1 presents a Venn diagram of this terminology hierarchy. AI describes algorithms that solve problems that usually require human intelligence. Machine learning is a subclass of AI, devoted to creating algorithms with the ability to learn without being explicitly programmed. Deep learning is the next subclass in the hierarchic terminology. The main difference between deep learning and classic machine learning is that in the latter, human experts choose imaging features that appear to best represent the visual data, while in deep learning, no feature selection is used. Instead, the deep learning algorithms learn on their own which features are best for the computational task. Most deep learning algorithms are based on artificial neural networks. A CNN is a subcategory of artificial neural network that makes the explicit assumption that the inputs are images. In the past few years, CNN technology has been the basis for some of the most influential innovations in the field of computer vision (5,15).

**Artificial neural networks.**—An analogy between the artificial neuron and the biologic neuron can contribute to the understanding of the underlying technology. The model of biologic neurons assumes that neurons typically consist of three parts: dendrites, a cell body, and an axon (Fig 2). Neurons receive input signals via the dendrites, and a “function” is performed in the cell body. If the final sum is above a certain threshold, the neuron outputs an action potential, sending a spike along its axon. In most synapses, signals are sent from the axon of one neuron to a dendrite of another.

Inspired by biologic neural systems, artificial neural networks are composed of multiple computational units called artificial neurons (Fig 2). An artificial neuron receives input signals  $x_1, x_2, \dots, x_n$ , which are multiplied by the synapses' strength, termed weights ( $\omega$ ). Parallel to the action potential firing in the

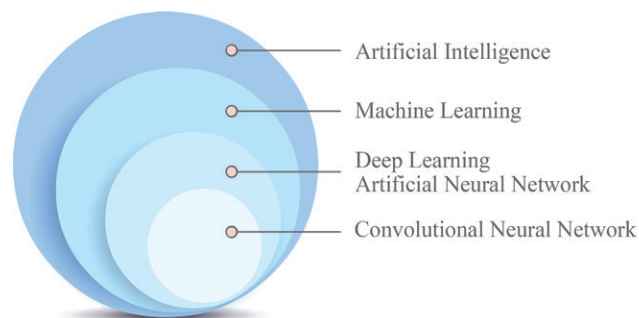


**Figure 1:** Venn diagram representation of convolutional neural networks in the artificial intelligence hierarchic terminology.

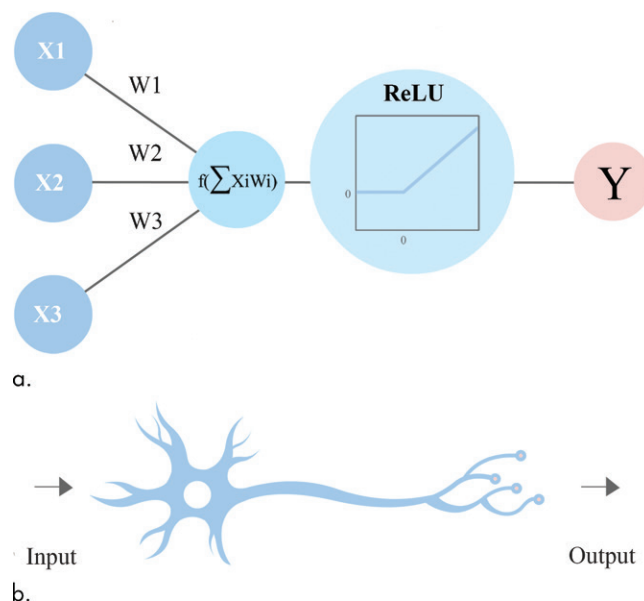


**Figure 2:** (a) Schematic representation of an artificial neuron shows its similarities to (b) a biologic neuron. Input of data is received through the dendrites, which are usually termed weights in the artificial neuron. Each input is multiplied by its corresponding weight, and all the multiplications are summed (dot product). A nonlinear mathematical formula is performed on the result. The most commonly used formula today is the rectified linear unit (ReLU) function. The output of the neuron serves as an input in the next layer of neurons.  $W$  = weight,  $X$  = input,  $Y$  = output.

cell, the activation function output determines the firing of neurons based on a weighted sum of its input. A nonlinear activation function  $f$  is applied to the sum of the multiplication of inputs and weights ( $\sum x\omega$ ). In the past, a common choice for activation function was the sigmoid function  $s(z) = 1/[1 + \exp(-z)]$ , which takes a real-valued input and “squashes” it to range between 0 and 1. At present, the most popular nonlinear function is the rectified linear unit (ReLU) function, a mathematical formula that chooses the maximum of either  $z$  or 0 and is designated as  $f(z) = \max(0, z)$ .

Artificial neural networks are modeled as collections of neurons that are connected in an acyclic graph where the outputs of some neurons can become inputs to other neurons. Neurons are arranged in multiple hidden layers in which neurons in adjacent layers have full pairwise connections, but neurons within a layer

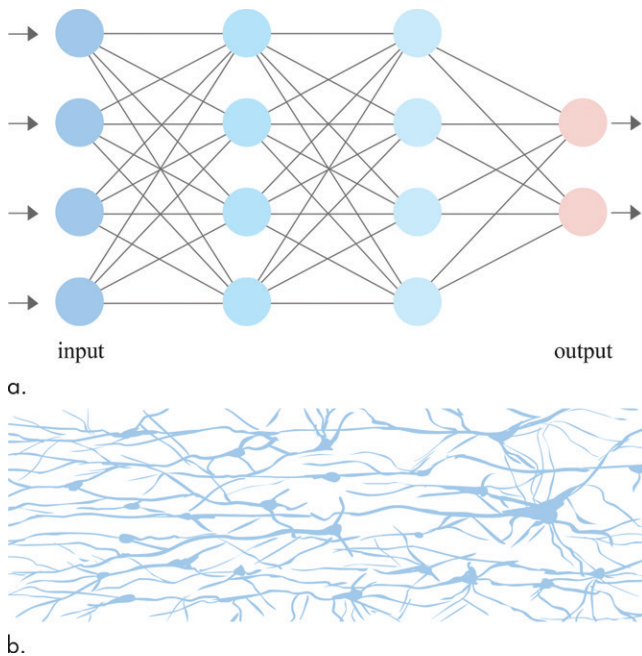


**Figure 3:** (a) Schematic representation of an artificial neural network and its similarity to (b) a biologic neural network. The strength of artificial neural networks resides in the integration of multiple neurons in the multiple deep hidden layers. The outputs of one layer serve as the inputs of the next layer. The last layer of neurons consists of a loss function, which estimates the current accuracy of the network in predicting the labels of specified data, a process called forward propagation. On the basis of the loss, small changes are conducted in the network's weights in a process called back propagation. Repeated iterations of forward and back propagation on the entire data set eventually produce an optimized network.

are not connected. Feedforward neural networks (Fig 3) learn to map a fixed-size input (eg, an image) to a fixed-size output (eg, a probability for each of several categories).

**CNN architecture.**—CNNs are very similar to artificial neural networks, with the explicit assumption that the inputs are images. This assumption allows us to encode certain properties into the CNN architecture. The typical CNN architecture is built of several layers that enable it to learn hierarchic feature representation of an image. Features in the first layer of representation typically represent the presence or absence of edges at particular orientations and locations in the image. The second layer typically detects motifs by spotting arrangements of edges, regardless of small variations in the edge positions. The third layer may assemble motifs into larger combinations that correspond to parts of familiar objects, and subsequent layers can detect objects as combinations of these parts.

The CNN architecture comprises a sequence of layers that transform the image volume into output class scores (Fig 4). Every layer transforms one volume of activations to another through a differentiable function. The main types of layers combined to build a CNN are the convolutional layer, the pooling layer, the nonlinearity layer, and the fully connected layer, which are discussed further below.

The convolution (CONV) layer is the core building block of a CNN. The CONV layer's parameters consist of a set of learnable filters. Each filter can be spatially small but extends through the full depth of the input volume. During the forward pass, each filter is convolved across the width and height of the input volume and computes dot products between the entries of the filter and the input at any position (Fig 5). As the filter slides over the input volume, a two-dimensional map is produced that provides the responses of that filter at every spatial position. One CONV layer contains a set of filters, and each filter will produce a separate map. The output volume is a stack of these maps along the depth dimension. Every entry in the output volume can thus also be interpreted as an output of a neuron that looks at a small region in the input and shares parameters with neurons in the same activation map.

The pooling layer usually performs down-sampling of the spatial dimension. It is common to periodically insert a pooling layer between successive CONV layers. The function of the pooling layer is to progressively reduce the spatial size of the representation to minimize the amount of parameters and computation in the network, as well as to control overfitting. The pooling layer operates independently on every depth slice of the input and resizes it spatially. The most common pooling function is the MAX pooling function, which uses the maximum value from each cluster of neurons at the prior layer to form a new neuron in the next layer. Other functions like average pooling are also applicable.

The nonlinearity layer is a layer that applies element-wise nonlinearity by using a specific activation function. As mentioned, the most common activation function is the ReLU function,  $f(z) = \max(0, z)$ , which is simply thresholded at zero.

The fully connected layer (also known as the dense layer) is a layer of neurons with full connections to all activations in the previous layer, as seen in classic neural networks. The CONV and pooling layers act as feature extractors from the input image, while the fully connected layer acts as a classifier. It is worth mentioning that we can implement a fully connected layer using a CONV layer by setting the filter size to be exactly the size of the input volume.

Although we can explain the process by which algorithms are mathematically constructed, a CNN is still considered to be a "black box," as it is difficult to determine how the network arrived at its conclusion. More information on the black box and strategies developed to understand what the CNN is responding to in the decision-making process has been presented in various articles (5,6,16).

### Deep Learning Study Design

Designing a deep learning study entails a common pattern that includes several steps. The initial step is the formulation of a clinical question. After establishing the clinical question, a suitable computer vision task is chosen, with its appropriate metrics. Subsequently, the stage of data acquisition and data preprocessing is addressed, and this includes planning of data for both training and testing and the annotation of medical data. Thereafter, the software framework and the hardware



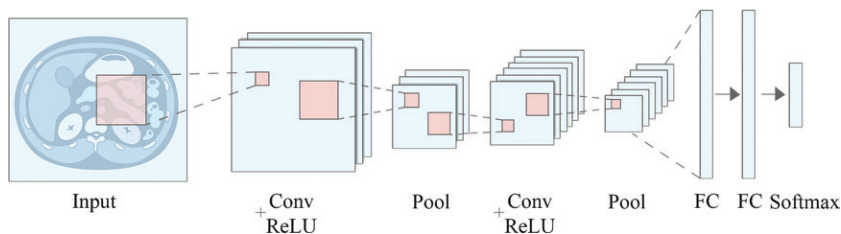


**Figure 4:** A typical convolutional neural network (CNN) architecture for image classification. CNN architecture comprises a sequence of layers that transform the image volume into output class scores. Every layer transforms one volume of activations to another through a differentiable function. There are four main types of layers that are combined to build a CNN: convolution (*Conv*), pooling (*Pool*), nonlinearity (rectified linear unit [*ReLU*]), and fully connected (*FC*) layers.

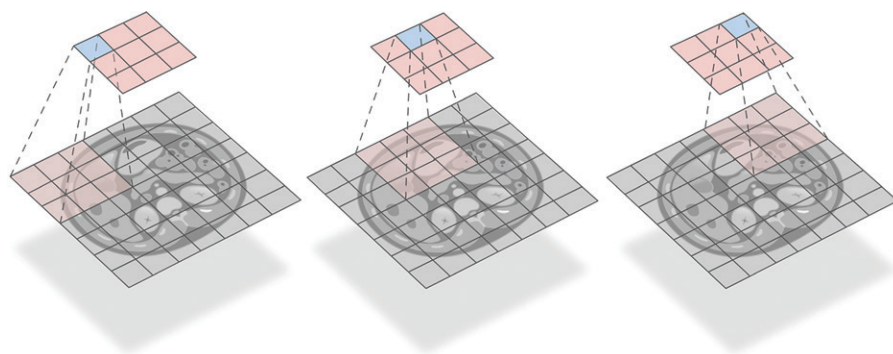


**Figure 5:** Illustration of a convolution from the input to output. The main difference between convolutional neural networks (CNNs) and regular artificial neural networks is the use of weight sharing in the former. Images are very large matrixes of pixels, and each pixel constitutes one input. Using separate weights for each pixel would be computationally taxing. Another characterization of images is the appearance of recurrent patterns. CNNs make use of this property. Each layer in the network consists of small matrixes of weights, also called filters. Each filter is systematically shifted along the image, so that in each area along the image a dot product is made between the pixels and the weights. The dot product between each filter and each specific region creates a neuron per pixel in the image.

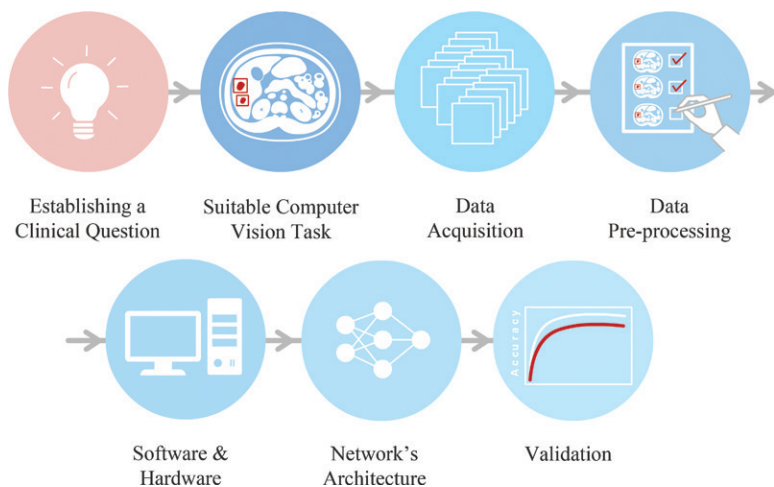


**Figure 6:** Diagram of the steps involved in constructing a deep learning study. The first step is to define a clinical question. A suitable computer vision task is then chosen. Thereafter, data acquisition and data preprocessing are generated. The engineering team selects the software framework and the hardware platform, and the network's architecture is designed. Last, the network is validated on the testing data. This research design emphasizes the cooperative effort between the clinical team and the engineering group so as to accomplish optimal results.

platform are selected, and the network's architecture is designed. Finally, the results are validated on the testing data using the chosen metrics. Each step of this process will be elaborated in the following subsections (Fig 6).

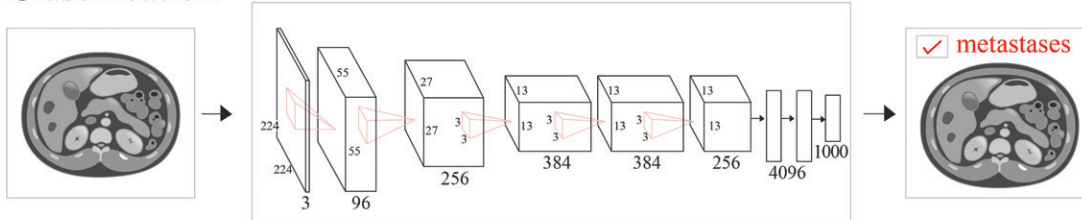
**Clinical question.**—The clinical question that is selected evolves from the various radiologic fields and the relevant imaging modalities. Clinical tasks are mostly based on the radiologists' experience and are generated from practical needs. When selecting a clinical task, it is important to ascertain that it can be applicable to the technologic deep learning solution. Deep learning has a distinct advantage when processing unstructured data, while classic machine learning may be preferred for data that are characterized as being well structured and having well-defined features (5).

**Computer vision tasks.**—Common computer vision tasks that are particularly applicable to the radiology field include classification, detection, and segmentation (5) (Fig 7). Another category that we have chosen to include as a network task is image optimization.

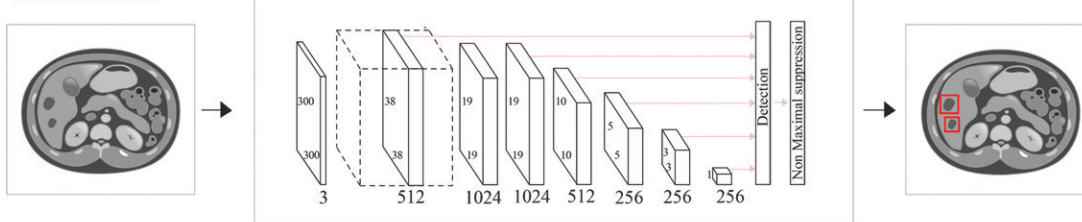
Classification is the task of categorizing or labeling an image into a specific class—for example, classifying chest radiographs as either normal or showing features of tuberculosis. This computer vision task is fundamental to accomplish further network tasks. Detection allows for the identification of the location of lesions, organs, or other objects of interest—for example, localizing the  $x, y$  coordinates of hepatic masses. Segmentation is implemented to define the precise pixel-wise boundaries of an organ or pathologic feature. Image optimization includes tasks such as the enhancement of image resolution, as well as the formulation of synthetic image input (17). It is important to note that the determination of a task as one of the above-defined labels is not always clear cut.

Each specific task makes use of a particular statistical method (metrics) to present the results. For example, classification results can be evaluated by using receiver operating characteristic curves, detection results can be measured by using true-positive rate and false-positive rate, and segmentation results can be estimated

### Classification



### Detection



### Segmentation

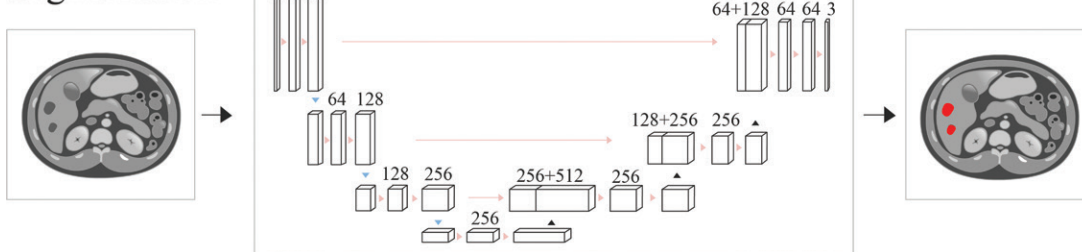


**Figure 7:** Three common tasks in computer vision include classification, detection, and segmentation. The labeling of the images depends on the required task. Classification requires image labeling. Detection requires marking of a region of interest, such as a boxplot. Segmentation requires pixel-wise delineation of the desired object. The complexity of the labeling increases from classification to detection to segmentation. In this image we present examples of popular networks. AlexNet (top) and VGG (middle) architectures are used for classification and detection, and U-Net (bottom) is the most commonly used network for segmentation.

by using the Dice coefficient or Jaccard index, two statistical methods that are used for comparing the similarity of two samples (5).

**Data acquisition.**—Training of deep networks relies on large data sets. The existing imaging data set in the medical world is more limited in comparison to the wider non-medical data sets in computer vision (6). Examples of two large nonmedical databases include the ImageNet database, which contains more than 14 million annotated images (18), and the CIFAR-10 database, which contains 60 000 annotated images (19).

Studies that have used deep learning in radiology are based on either a private data set or a publicly available data set. The use of a public database offers the opportunity for collaboration between researchers in the academic community. In addition, the public data sets are annotated to allow for a uniform label to evaluate the algorithm performance. Once the data are acquired, they are then split into training and testing sets. More information on the topic of splitting data sets can be found in an article by Park and Han (20).

**Preprocessing of data.**—An important point in medical image analysis is data preparation. Manual labeling and annotation are time consuming. Several options can be used for the process of data preparation and include the following, in increasing order of complexity: (a) image labeling (eg, “radiograph with tuberculosis”); (b) region of interest (ROI) markings, such as square or circular ROIs; and (c) pixel-wise segmentation. Different computer vision tasks require different annotations. For example, organ or pathologic feature segmentation requires laborious pixel-wise segmentation, while classifying chest radiographs as either showing tuberculosis or normal requires only image labeling and thus may potentially allow the use of a larger cohort.

Data augmentation is a technique used to overcome the obstacle of a limited training data set. Augmentation is implemented to artificially increase the number of training images. This is accomplished by using various combinations of multiple transformations that include techniques such as image rotation and image flipping. A substantial machine learning obstacle is overfitting, whereby a model is unable to generalize patterns beyond the training set. With data augmentation,

more data are created, and thus the model becomes more robust for independent information on the testing set.

**Hardware and software.**—The next step in the research design process is the selection of a hardware platform and a software framework. Deep learning has been made possible by the development of novel hardware technology, which allows for the highly rapid processing of matrix operations. The introduction of the graphics processing unit, or GPU, has opened the possibility of training large networks in an effective and time-saving manner. Parallel to hardware development, sophisticated software tools have also been created that have enabled the formation of deep neural networks. These open-source frameworks have eased the programming of neural networks (21,22). Popular packages include the following:

- Caffe (23), which was developed by Berkeley Vision and Learning Center and supports interfaces like C, C++, Python, and MATLAB.
- TensorFlow (24), created by Google, which supports languages such as Python, C++, and R.
- Torch (25), a package developed and maintained by Ronan Collobert, Koray Kavukcuoglu, and Clement Farabet that is a Lua-based deep learning framework used by Facebook, Twitter, and Google.
- Keras (26), developed by François Chollet and designated as a third-party package, as it is capable of running on top of TensorFlow or Theano.

**Architecture.**—The CNN architecture defines the structure of the layers of the neural network. Although there are various forms of CNN architectures, they are generally based on a repeated pattern of sequences. As discussed above, the architecture includes an input layer, hidden learning layers (which in most cases consist of convolutional and pooling sublayers), and an output layer (15). Different tasks require different network architectures, and choosing the appropriate architecture can improve the overall performance. Researchers can choose to make use of previously developed CNN models, or they can construct their own “in-house” architecture (4,27–29). Popular architectures include the following:

- AlexNet (4), which is a classification architecture consisting of five convolutional layers that was developed by Alex Krizhevsky, Ilya Sutskever, and Geoffrey Hinton and was awarded first place in the ImageNet Large Scale Visual Recognition Challenge in 2012.
- VGG16/VGG19 (28), which represent architectures consisting of 16 and 19 layers, respectively. This architecture was developed by Karen Simonyan and Andrew Zisserman and won first place in the ImageNet challenge of 2014.
- U-Net (29), a segmentation architecture formulated of a contracting path and an expansive path that substitutes the fully connected layers and allows fewer training images and yields more accurate segmentations. This architecture was developed by Olaf Ronneberger at the University of Freiburg.

The input data for CNN can be either a two-dimensional matrix or a three-dimensional tensor. In a large portion of

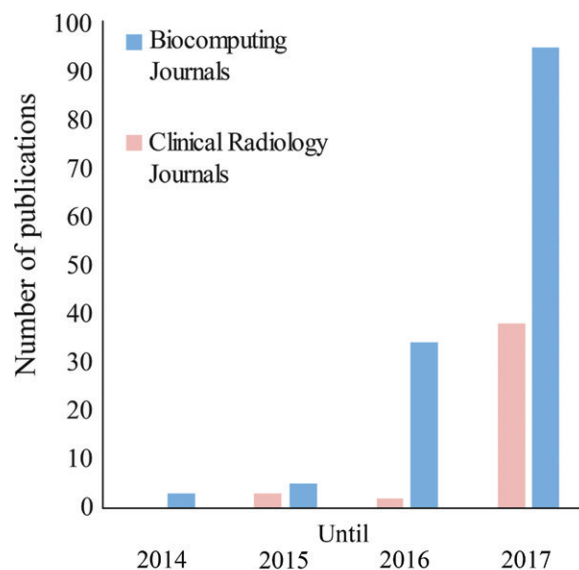


**Figure 8:** Bar graph shows the trend of deep learning radiology articles published in recent years. A growth trend has occurred recently in clinical radiology journals compared with biocomputing journals.

medical images, the data are in the form of three-dimensional volumes. When analyzing the volumetric data, a two-dimensional CNN architecture can be used; however, the use of a single-section analysis may lead to the loss of important volumetric information. The disadvantage of this approach can be overcome by using a direct three-dimensional CNN architecture. This, however, is at the expense of a much higher computational cost.

CNN predefined architectures, such as AlexNet or VGG, may be pretrained on large-scale data sets such as ImageNet before training on the small specific medical data set of interest (30,31). This method, referred to as pretraining or transfer learning, is currently widely implemented in the deep learning medical world and may alleviate the limitation of small data sets. Transfer learning can be understood by examining human behavior: When a person confronts a novel task, he or she transfers information that is accumulated from other fields of knowledge. While in nontransfer learning, all the weights are randomly assigned in the pre-training phase, in transfer learning, the weights of layers of the network are derived from training on the nonmedical large-scale data. There are variations in transfer learning regarding how many layers should be retrained with medical data and whether the weights in the layers to be retrained should be fine-tuned or trained from scratch.

**Validation.**—In machine learning, and specifically in deep learning, a validation technique is adopted to formulate a predictive model that is able to evaluate the system’s ability to generalize to an independent set of data. Two common types of validation methods include the holdout method and the k-fold cross-validation method. In the holdout method, data are randomly subdivided into training, validation, and testing sets.

**Table 1: Reviewed Articles according to Deep Learning Study Design**

Stage in Deep Learning Research Design	Frequency of Implementation
Stage 1: clinical question	Top three investigated organs: brain (22%), chest (18%), abdomen/pelvis (16%); top three investigated modalities: MRI (35%), CT (26%), mammography (11%)
Stage 2: computer vision task	Task implementation: classification (43%), segmentation (29%), detection (19%), image optimization (9%)
Stage 3: data acquisition	Data set size: ≤100 cases (25%), 101–1000 cases (49%), 1001–10 000 cases (20%), >10 000 cases (6%); type of data set: private (64%), public (27%), private and public (9%)
Stage 4: data preprocessing	Type of annotation: pixel-wise segmentation (44%), image labeling (29%), ROI (27%); data augmentation: implemented by 51% of the studies
Stage 5: hardware and software	Type of hardware: NVIDIA GPU (99%), CPU (1%); top three libraries: Caffe (23%), Theano (11%), Keras (7%)*
Stage 6: architecture	Top three networks: AlexNet (18%), VGG (11%), GoogLeNet (9%) <sup>†</sup> ; 3D CNN architecture: implemented by 15% of the studies <sup>‡</sup> ; transfer learning: implemented by 30% of the studies
Stage 7: validation	Type of validation: holdout method (58%), k-fold cross validation (42%)

Note.—CNN = convolutional neural network, CPU = central processing unit, GPU = graphics processing unit, ROI = region of interest, 3D = three-dimensional.

\* Only 112 (62%) of 180 articles specified the hardware solution that was implemented.

<sup>†</sup> Eighty-eight (48%) of 180 studies used an “in-house” network.

<sup>‡</sup> One hundred seventeen (65%) of 180 studies used volumetric data.

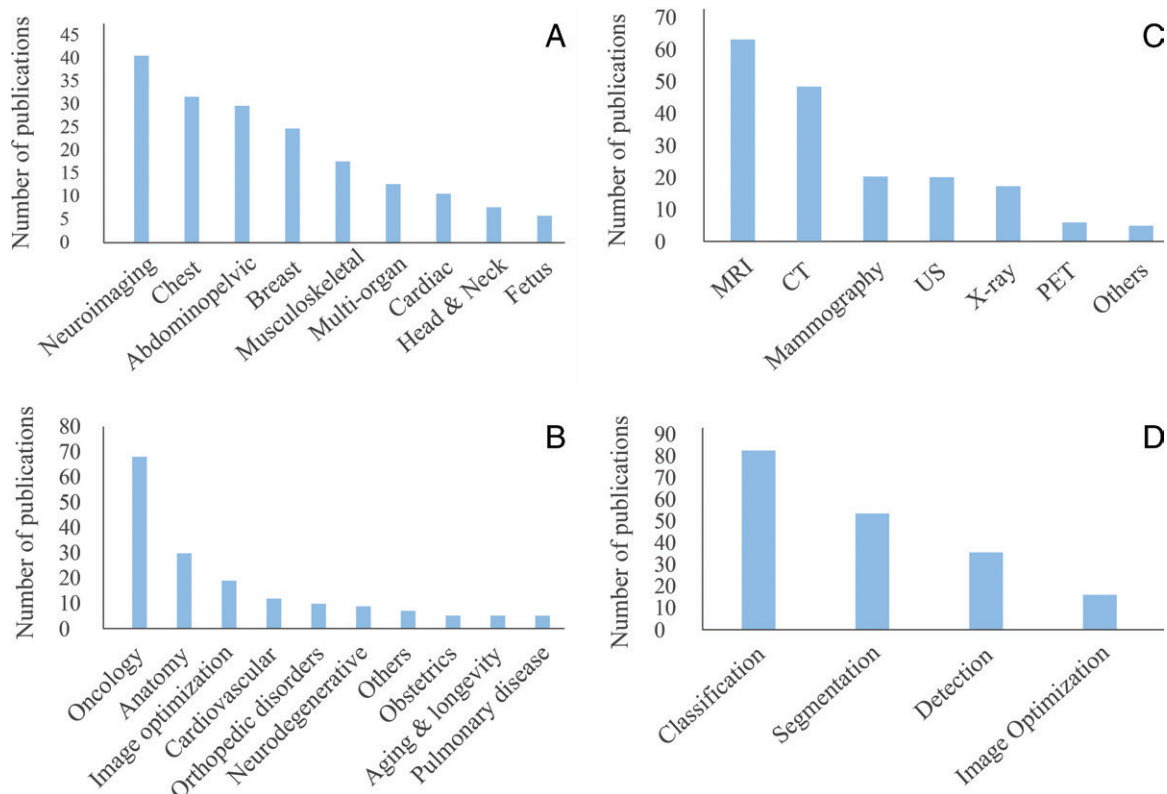


**Figure 9:** Histograms show the categorization of the reviewed articles in our report according to studied, A, organ systems, B, type of pathologic finding, C, image modality, and, D, the various computer vision tasks.

In the k-fold cross validation method, the data are partitioned into *k* nonoverlapping subsets. The training and validation process is performed *k* times, during which the *k* subsets take turns in serving as the validation set while the remaining (*k* – 1) subsets are used together as the training set in each of the *k* cycles (32,33).

For any machine learning model, after the training and validation optimization is performed, it is crucial to validate the performance of the trained model with an independent test set that has not been seen by the model during the training and validation process. The use of independent testing is an important step before a model can be considered to be generalizable to the population.



## Literature to Date of CNN Studies in Radiologic Imaging

### Literature Search

A search of the published literature was performed by using PubMed for the key words (“deep learning” OR “convolutional neural network”) AND (“image” OR “imaging” OR “radiology”). All peer-reviewed original publications in journals, as well as in conference proceedings, that were published between January 2013 and January 2018 in the subject of CNN application in image radiology analysis were included. The year 2013 was chosen as a starting point for inclusion, as this was the period that followed the initial acknowledgment of the CNN in the computer vision community (4). We excluded articles that focused on the implementation of CNN to nonradiologic medical images.

Although we performed a broad search, we are aware that we were not able to include all the published data. We focused on PubMed as our search engine, although other electronic databases, such as arXiv, are available. PubMed is a central database that is widely used by the medical community, and despite the fact that it does not contain all written work on this subject, it nevertheless covers the prominent issues in this field. In addition, deep learning is a dynamic topic, and rapid changes in this field are continuously occurring. Because our database stems from peer-reviewed journals, it is important to take into account that the information presented in the articles may reach the reader at a delay.

### Literature Search Results

The search results produced 744 articles, of which 180 were found to be relevant. Figure 8 shows the trend of deep learning radiology articles published in recent years. Each article was examined according to the deep learning research design that was presented above (Table 1).

When we analyzed the reviewed articles, we found it interesting to note the organs and imaging modalities that were involved, as well as the types of pathologic findings. Neuroimaging and MRI were shown to be the most common selections for CNN research (Fig 9, *A* and *C*); moreover, the field of oncology was the most frequently investigated disease (Fig 9, *B*). The most prevalent selection for computer vision task was classification (Fig 9, *D*). In addition, we examined the data set size according to the type of annotation (Fig 10). About 95% of the studies used data sets with fewer than 10 000 cases. Seventy percent of the studies with more than 10 000 cases used image labeling for annotation.

The following section presents a summary of the applied deep learning research in radiology divided by the top five investigated major organ systems: neurology, chest, abdomen and pelvis, breast, and musculoskeletal system. For each topic, we have chosen to present one or two prominent studies that were found to be clinically influential. Tables 2–4 summarize various clinical tasks that were investigated according to the relevant organ or organ system.

**Neuroimaging.**—Neuroimaging deep learning research has primarily focused on neuroanatomic structure segmentation (41–43). One prominent network (41) is aimed at segmenting the brain into four class structures: gray matter, white matter,

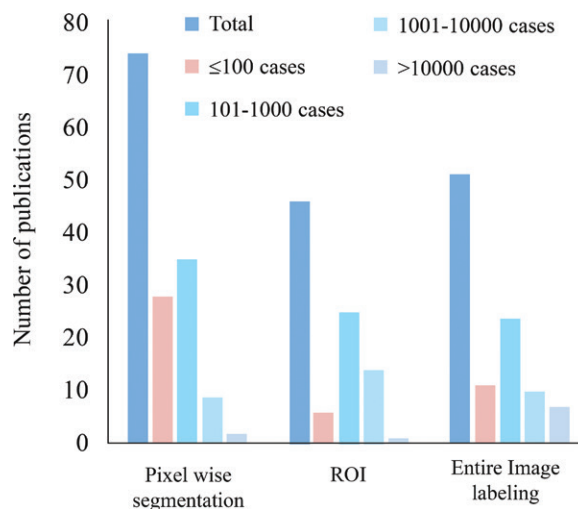


**Figure 10:** Histogram shows the relationship between annotation type and data set size. In each type of annotation and labeling, we can see the total number of cases, as well as their distribution into various ranges according to the number of cases used. ROI = region of interest.

cerebrospinal fluid, and background at MRI. The study used a public data set, the Medical Image Computing and Computer Assisted Intervention, or MICCAI, Society MRBrainS (Table 5) data set, which contains 20 segmented MRI studies, and showed Dice coefficients of 0.84–0.89 for the different structures. Further works have presented CNN research on brain lesions with a focus on glioma tumor segmentation (52–54). Academic endeavors have also presented several works in the classification of neurodegenerative diseases. CNN technology has been implemented for the classification of Alzheimer disease and mild cognitive impairment on MR images and CT scans for a noninvasive biomarker to determine which patients may benefit from early treatment. These works utilized the Alzheimer’s Disease Neuroimaging Initiative public database (Table 5) (34,35).

**Chest.**—Deep learning has been used for the detection and classification of chest abnormalities, including cancer, parenchymal lung disease, and infectious disease. The most prevalent task is the detection and classification of lung nodules in chest radiographs and in CT scans (101–106,111). The LUNA16 is an example of a challenge using the public Lung Image Database Consortium–Image Database Resource Initiative data set (Table 5) for pulmonary nodule detection. For the classification task, most research groups directly categorized nodules as either malignant or non-malignant, whereas few investigators chose to characterize nodules according to radiologic features such as nodule density, calcification, and location (101,102). CNN methods have also been developed for the classification of parenchymal lung disease, including interstitial lung disease patterns and chronic obstructive pulmonary disease (121–123). Other research utilizing a large private data set (35 038 radiographs) classified radiographs as either normal or showing one of the following pathologic features: cardiomegaly, consolidation, pleural effusion, pulmonary edema, or pneumothorax. This algorithm had areas under the receiver operating charac-



**Table 2: A Summary of Various Clinical Tasks That Were Investigated in Neuroimaging as Well as in the Musculoskeletal System**

Organ System and Classification	Detection	Segmentation	Image Technique and Image Optimization
<b>Neurologic system</b>			
Classification of AD/MCI (at MRI, CT, PET/CT) (34–39)	Brain anatomic landmarks (at MRI) (40)	Brain anatomic structures (at MRI) (41–48)	“Skull stripping” (at MRI) (49)
Identification of PD (with brain SPECT) (50)	Brain hyperperfusion (at MRI) (51)	Brain tumors (at MRI) (52–56)	MRI-based synthetic CT generation (57)
Prediction of tissue necrosis after CVA (at MRI) (58)	Cerebral aneurysms (at MRI) (59)	Brain stroke (at MRI) (53,60,61)	Reduction of diffusion MRI data processing to a single optimized step (62)
Characterization of carotid plaque composition (at US) (63)	Cerebral microbleeds (at MRI) (64)	Traumatic brain injury (at MRI) (53)	Multimodal MRI sequence synthesis (65)
Identification of isocitrate dehydrogenase 1 mutation status in low-grade glioma (at MRI) (66,67)	...	Multiple sclerosis lesions (at MRI) (68)	Generation of arterial spin-labeling perfusion images by using a smaller number of subtraction images (at MRI) (69)
Classification of GBM methylation according to the O6-methylguanine methyltransferase gene status (at MRI) (70,71)	...	Organs at risk at head and neck CT (72)	...
Overall survival prediction for GBM (at MRI) (73,74)	...	Thyroid nodules at US (75,76)	...
Prediction of brain age (at MRI) (77)	...	Infant brain tissue at MRI (78)	...
Identification of alcoholism in the brain (at MRI) (79)	...	...	...
Classification of thyroid nodules (at US) (80,81)	...	...	...
<b>Musculoskeletal system</b>			
Bone age assessment (at radiography) (82–85)	Spinal disk and vertebral pathologic findings at MRI (86)	Knee joint cartilage or bone at MRI (87,88)	...
Identification of hip osteoarthritis (at radiography) (88)	Vertebra labeling (at CT, MRI, radiography, US) (89–93)	Skeletal muscle at CT (94)	...
Identification of myositis (at US) (95)	Vertebral metastases at MRI (96)	Adipose tissue at CT (97)	...
Classification of histopathologic subtypes of rhabdomyosarcoma at MRI (98)	L3 slice at CT (99)	...	...
Identification of wrist, hand, and ankle fractures (at radiography) (100)	...	...	...

Note.—AD = Alzheimer disease, CVA = cerebrovascular accident, GBM = glioblastoma multiforme, MCI = mild cognitive impairment, PD = Parkinson disease, SPECT = single photon emission computed tomography.

teristic curve of 0.850–0.962 for the different findings (134). Additional work on radiographs has evaluated CNN methods for the detection of pulmonary tuberculosis (129,130).

**Abdomen and pelvis.**—Abdominopelvic imaging analysis using deep learning has mainly focused on organ segmentation (eg, liver, spleen, kidney, urinary bladder, and prostate) on CT scans and US images (40,118,137,174,175,181,183,190,193). Many deep learning studies have focused on the liver. In addition to liver segmentation, other studies have investigated the classification of liver pathologic findings, includ-

ing classification of liver lesions at CT (172), classification of liver metastases according to the primary origin site (178), and staging of liver fibrosis at MRI (194). Other abdominopelvic oncologic research has evaluated prostate, bladder, and rectal cancer (182,191,195). Research on the application of CNNs to gastrointestinal pathologic findings is still scarce; one study classified small-bowel obstruction on radiographs (185), and another study detected colitis at CT (186).

**Breast.**—The most commonly researched CNN application in breast imaging is detection and classification of breast cancer at

**Table 3: A Summary of Various Clinical Tasks That Were Investigated in Chest Imaging, Cardiac Imaging, and Obstetrics**

Organ System and Classification	Detection	Segmentation	Image Technique and Image Optimization
<b>Chest</b>			
Classification of lung nodules at CT (101–110)	Lung nodules (at radiography, CT, PET/CT) (111–114)	Vessel segmentation (at angiography) (115)	Bone suppression (at radiography) (116)
Classification of mediastinal lymph nodes (at PET/CT) (117)	Mediastinal lymph nodes at CT (118)	Lung nodules at CT (119)	Enhancement of image resolution in chest CT (120)
Classification of parenchymal pulmonary disease at CT (121–125)	Peripherally inserted central catheter tip location at radiography (126)	Anatomic structures at CT (127,128)	...
Identification of tuberculosis at radiography (129,130)	Longevity prediction at CT (131)	...	...
Classification of PA and lateral radiographs (132)	...	...	...
Predicting response to neoadjuvant chemotherapy in esophageal cancer at PET (133)	...	...	...
Classification of chest radiographs according to common findings (134)	...	...	...
<b>Cardiac imaging</b>			
Quality assessment of echocardiograms (135)	Identification and quantification of coronary artery calcification at CT (136)	Cardiac structures at MRI (137–139)	...
Identification of end-diastole and end-systole frames at MRI (140)	...	Reconstruction of 2D cardiac MR images (141)	...
Classification of coronary artery stenosis at CT (142)	...	...	...
<b>Obstetrics</b>			
Recognition of fetal facial standard plane at US (143)	...	Fetal brain tissue at MRI (144)	...
Recognition of fetal abdominal standard plane at US (145)	...	Fetal body and amniotic fluid at US (146)	...

Note.—PA = posterioranterior, 2D = two-dimensional.

mammography (147–151,159–161,166,204). Parameters that are similar to those adopted by radiologists have been incorporated by some researchers, including symmetry differences, temporal changes (160), and detection of microcalcifications (166). For classification, most researchers have focused on benign versus malignant lesion differentiation, and some studies have categorized images according to the Breast Imaging Reporting and Data System, or BI-RADS, score (168). More recently, several investigations have implemented a more holistic approach (150,151). For example, a study (150) using the public data sets INbreast and the Digital Database for Screening Mammography (Table 5) for 1090 scans presented an algorithm that generated segmentation maps from breast lesions as well as from microcalcifications and concurrently classified the entire scan. This algorithm provides a complete automated method for mammography analysis, with an area under the receiver operating characteristic curve of 0.86.

**Musculoskeletal system.**—Prominent investigated musculoskeletal imaging tasks include bone age assessment (82–85), spine level detection (89–92), spinal orthopedic pathologic find-

ing detection (86), osteoarthritis detection (87,88,205), and fracture detection (100). A popular musculoskeletal task is bone age assessment, which has been the focus of several studies (82–85). Although classic machine learning tools for skeletal maturity assessment have been commercially available, novel research endeavors are focused on the implementation of CNNs on skeletal maturity tasks. One prominent study (82) has developed a CNN-based system using a large private database of 12 000 radiographs of the left hand and has demonstrated that the CNN showed similar accuracy to both an expert radiologist and the available automated non-CNN programs. Researchers have also focused on a need to accurately identify the correct vertebra level and have applied CNN for various image modalities, including MRI, CT, and radiography (89–92).

## Future Trends

As we have seen in our review, the majority of studies have concentrated on one specific computer vision task such as classification, detection, or segmentation. For example, many chest imaging (111–113) and breast imaging (159–164) studies deal

**Table 4: A Summary of Various Clinical Tasks That Were Investigated in the Breast, in the Abdomen and Pelvis, and in Multiorgan Systems**

Organ System and Classification	Detection	Segmentation	Image Technique and Image Optimization
<b>Breast</b>			
Classification of breast lesions (at MG, US, MRI, TS) (147–158)	Breast lesions (at MG, US, TS) (151,159–164)	Breast lesions at MG (151)	...
Classification of breast parenchyma into normal and high risk at MG (165)	Breast microcalcifications at MG (166)	Breast fibroglandular tissue at MRI (167)	...
Classification of breast density categories at MG (168–170)	Breast calcified arteries at MG (171)	...	...
<b>Abdomen and pelvis</b>			
Classification of liver lesions at CT (172)	Liver tumors at follow-up CT (173)	Liver and liver lesions (at CT, MRI) (137,174–176)	Pelvic image de-noising and contrast enhancement (at radiography) (177)
Classification of liver metastases into the primary site of origin at CT (178)	Prostate landmarks at CT (40)	Portal vein at CT (179)	Screening of T2-weighted liver acquisitions for nondiagnostic images at MRI (180)
Classification of abdominal organs at US (181)	Prostate cancer at MRI (182)	Prostate at MRI (183)	Pseudo-CT generation from pelvis MRI and PET/MRI (184)
Identification of bowel obstruction at radiography (185)	Colitis at CT (186)	Kidney and polycystic kidney at CT (174,187)	...
Identification of cirrhosis at US (188)	Abdominal LN at CT (118)	Spleen at CT (174)	...
Bladder cancer treatment response assessment at CT (189)	...	Urinary bladder and bladder cancer at CT (190,191)	...
Identification of prostate cancer at MRI (192)	...	Pancreas at CT (193)	...
Liver fibrosis staging at MRI (194)	...	Rectal cancer at MRI (195)	...
<b>Multiorgan systems</b>			
Identification of motion artifacts at MRI (196)	Localization of anatomic structures at CT (197)	Tumor segmentation at PET/CT (198)	Reconstruction of low-dose CT images (199–201)
...	...	...	Registration of a 3D radiography map provided by CT with a 2D radiography image in real time (202)
...	...	...	Retrieval of medical images having visual and semantic similarities at radiography (203)

Note.—LN = lymph node, MG = mammography, 3D = three-dimensional, TS = tomosynthesis, 2D = two-dimensional.

with the detection of nodules and masses. Tools for automatic lesion detection can be integrated into picture archiving and communication systems and can help radiologists in the process of image interpretation.

In the coming years, we expect researchers to adopt a holistic approach in which they simultaneously perform several computer vision tasks, whereby the algorithm will provide a fully automatic solution. For example, new breast imaging CNN studies present a holistic approach that mimics the radiologist's work (150,151), providing a completely automated method for lesion detection and classification in mammograms. In the past, machine learning computer-aided diagnosis systems for breast

cancer detection have been approved by the U.S. Food and Drug Administration, but there has been disagreement about whether they have been able to contribute to the radiologists' work (206). Using the holistic approach and the implementation of new CNN studies may improve the detection and classification process of breast lesions.

An interesting task that is scarcely implemented in current literature, to our knowledge, is the use of deep learning to obtain information that is beyond the radiologists' interpretation. An example of a study that adds data to the interpretation of medical images is the research on liver fibrosis quantification at MRI (194). Future advancement in this field will allow for greater

**Table 5: Public Data Sets Used in the Reviewed Studies**

Type of Repository and Collection	Web Page	Organ System	Image Modality	Data
<b>Public database</b>				
Indiana University Chest X-ray Collection	<a href="http://openi.nlm.nih.gov/">http://openi.nlm.nih.gov/</a>	Chest	Radiography	A total of 3996 radiology reports from the Indiana Network for Patient Care and 8121 associated images
The standard digital image database with and without chest lung nodules (JSRT database)	<a href="http://db.jsrt.or.jp/eng.php">http://db.jsrt.or.jp/eng.php</a>	Chest	Radiography	A total of 154 nodule images and 93 non-nodule images
The Lung Image Database Consortium image collection (LIDC-IDRI)	<a href="https://wiki.cancerimagingarchive.net/display/Public/LIDC-IDRI">https://wiki.cancerimagingarchive.net/display/Public/LIDC-IDRI</a>	Chest	CT	A total of 1018 cases with annotated nodules
A collection of cases with ILDs (ILD Database)	<a href="http://medgift.hevs.ch/wordpress/databases/ild-database/">http://medgift.hevs.ch/wordpress/databases/ild-database/</a>	Chest	CT	Multimedia database of findings in 128 patients with one of the 13 histologic diagnoses of ILDs
DDSM: Digital Database for Screening Mammography	<a href="http://marathon.csee.usf.edu/Mammography/Database.html">http://marathon.csee.usf.edu/Mammography/Database.html</a>	Breast	MG	Approximately 2500 cases—each study includes two images of each breast
INbreast mammographic database	<a href="http://medicalresearch.inescporto.pt/breastresearch/index.php/Get_INbreast_Database">http://medicalresearch.inescporto.pt/breastresearch/index.php/Get_INbreast_Database</a>	Breast	MG	A total of 115 cases with several types of lesions (masses, calcifications, asymmetries, and distortions); accurate contours made by specialists are also provided
Breast Cancer Digital Repository (BCDR)	<a href="https://bcdr.eu/information/about">https://bcdr.eu/information/about</a>	Breast	MG, US	Mammography and US images in 1734 patients that include information on clinical history, lesion segmentation, and selected pre-computed image-based descriptors
The Alzheimer's Disease Neuroimaging Initiative (ADNI)	<a href="http://adni.loni.usc.edu/">http://adni.loni.usc.edu/</a>	Brain	MRI, PET	Data in 650 patients with MCI, 350 patients with AD, and 350 elderly control subjects
The Parkinson's Progression Markers Initiative (PPMI)	<a href="http://www.ppmi-info.org/">http://www.ppmi-info.org/</a>	Brain	MRI, PET, SPECT	Data in 431 patients with PD, 193 healthy control subjects, and 77 patients with scans without evidence of dopamine deficit
The Internet Brain Segmentation Repository (IBSR)	<a href="https://www.nitrc.org/projects/ibsr/">https://www.nitrc.org/projects/ibsr/</a>	Brain	MRI	Includes 18 sets of MRI data with complete expert segmentations
The LONI Probabilistic Brain Atlas (LPBA40)	<a href="http://www.loni.usc.edu/atlas/Atlas_Detail.php?atlas_id=12">http://www.loni.usc.edu/atlas/Atlas_Detail.php?atlas_id=12</a>	Brain	MRI	Includes 40 MRI studies with segmentations of a set of 56 structures in the brain
The Open Access Series of Imaging Studies (OASIS)	<a href="http://www.oasis-brains.org/">http://www.oasis-brains.org/</a>	Brain	MRI	A collection of MRI studies in 416 subjects aged 18–96 years
Autism Brain Imaging Data Exchange (ABIDE)	<a href="http://fcon_1000.projects.nitrc.org/indilabide/">http://fcon_1000.projects.nitrc.org/indilabide/</a>	Brain	MRI	Data in 1112 cases, including 539 individuals with autism spectrum disorder (ASD) and 573 control subjects
Disk-degeneration linked pathologies (GENODISC)	<a href="http://www.physiol.ox.ac.uk/genodisc/index.html">http://www.physiol.ox.ac.uk/genodisc/index.html</a>	Spine	MRI	Consists of 12018 individual disk volumes, from 2009 patients
Platform for research on spinal imaging and image analysis (SpineWeb)	<a href="http://spineweb.digitalimaging-group.ca/spineweb/index.php?action=home">http://spineweb.digitalimaging-group.ca/spineweb/index.php?action=home</a>	Spine	CT, MRI	Includes data on vertebral segmentation, intervertebral disk localization and segmentation, and segmentation and classification of fractured vertebrae
Cartilage and bone segmentation from knee MRI data (SK110)	<a href="http://www.ski10.org/">http://www.ski10.org/</a>	Knee	MRI	A total of 150 segmented knee joint cases
The Digital Hand Atlas Database	<a href="https://ipilab.usc.edu/research/baaaweb/">https://ipilab.usc.edu/research/baaaweb/</a>	Hand	Radiography	A total of 1391 left-hand radiographs in children up to 18 years of age

**Table 5 (continues)**



**Table 5 (continued): Public Data Sets Used in the Reviewed Studies**

Type of Repository and Collection	Web Page	Organ System	Image Modality	Data
Left Ventricle Segmentation Challenge (LVSC)	<a href="http://www.cardiacatlas.org/challenges/lv-segmentation-challenge/">http://www.cardiacatlas.org/challenges/lv-segmentation-challenge/</a>	Cardiac	MRI	A total of 200 segmented myocardium cases
An open-access database of thyroid US images (DDTI)	<a href="http://cimalab.intec.col?lang=en&amp;mod=project&amp;id=31">http://cimalab.intec.col?lang=en&amp;mod=project&amp;id=31</a>	Thyroid	US	A total of 99 cases and 134 images; each case is presented as an XML file with the expert's annotation and the patient's information
Data set collections				
The Cancer Imaging Archive (TCIA)	<a href="http://www.cancerimagingarchive.net/">http://www.cancerimagingarchive.net/</a>	Multiorgan	Multimodality	The image data in TCIA are organized into purpose-built collections of subjects. The subjects typically have a cancer type and/or anatomic site (lung, brain, etc) in common.
MICCAI challenges	<a href="https://grand-challenge.org/all_challenges/">https://grand-challenge.org/all_challenges/</a>	Multiorgan	Multimodality	Data sets designated for machine learning challenges within the area of medical image analysis

Note.—AD = Alzheimer disease, IDRI = Image Database Resource Initiative, ILD = interstitial lung disease, JSRT = Japanese Society of Radiological Technology, LONI = (University of Southern California) Laboratory of Neuro Imaging, MCI = mild cognitive impairment, MICCAI = Medical Image Computing and Computer Assisted Intervention, MG = mammography, SKI10 = Segmentation of Knee Images 2010.

creativity and will introduce innovation and imagination to the application of this computer technique to the medical world, targeting tasks that are beyond the capabilities of human experts.

When formulating an interpretation, the radiologist must take into consideration a wide range of parameters, such as demographic factors, the patient's diagnosis, previous test results, and reasons for referral. In our review, we noticed few studies that incorporated meta-information into the image analysis (160,173,178). New directions in deep learning may expand this focus on analysis that is based not only on images but also on an input of a broad scope of relevant factors that are taken into account by the radiologist.

Today most of the published research is based on programming of networks by engineers according to clinical problems raised by radiologists. Few studies (159,207) are based on existing dedicated toolkits that make use of neural networks without the need for explicit programming. As deep learning is gaining popularity, it seems that there is room for new dedicated platforms that will promote machine learning research. A promising project is Google's cloud AutoML Vision, which aims to provide machine and deep learning products that enable developers with limited machine learning expertise to train models (208).

A known limitation of deep learning research in radiology is the scarcity of annotated data. In our review, we noticed that the majority of studies used data sets with fewer than 10000 cases. Most of the studies with more than 10000 cases used image labeling for annotation. Several methods have been adopted to overcome the challenge of limited data. One solution is the development of publicly available databases. We expect to see larger and more sophisticated public data sets as the interest in computer vision is increasing. The trend of data expansion is evident by the more than 100000 labeled chest radiographs that were released to the public by the National Institutes of Health in September

2017 (209). The labels in this database were formulated by using natural language processing (NLP) to derive information regarding disease classification from the radiologic reports. Methods that use free-text analysis, such as NLP, allow for the implementation of a larger database so that the stage of labeling can be omitted. An additional strategy that can be applied to overcome the phase of labeling is the implementation of an unsupervised method that is used independently or that is incorporated into supervised strategies. An example of an unsupervised strategy that has been applied is generative adversarial networks (210); the value of unsupervised learning alone is still undetermined.

In conclusion, a convolutional neural network (CNN) is an artificial intelligence algorithm that presents remarkable capabilities for image analysis. Recently, there has been a great deal of interest in using this technology in radiologic research, and the number of deep learning radiology publications is dramatically increasing and encompasses the major organ systems and imaging modalities. CNN studies show a general framework pattern according to the clinical question, computer vision tasks, data acquisition and preprocessing, hardware and software requirements, network architecture, and the validation of the results. At present, the application of CNNs to the clinical field is limited mostly to research. Nonetheless, current studies on this subject are of crucial importance, as they can potentially prove to be a stepping stone for advancing health care.

**Acknowledgment:** We thank Seth Rabinowitz, who provided insight and expertise in artificial intelligence that greatly assisted the study.

**Disclosures of Conflicts of Interest:** S.S. disclosed no relevant relationships. A.B. disclosed no relevant relationships. O.S. disclosed no relevant relationships. M.M.A. disclosed no relevant relationships. H.G. disclosed no relevant relationships. E.K. disclosed no relevant relationships.

## References

- Kruskal JB, Berkowitz S, Geis JR, Kim W, Nagy P, Dreyer K. Big data and machine learning-strategies for driving this bus: a summary of the 2016 Intersociety Summer Conference. *J Am Coll Radiol* 2017;14(6):811–817.
- Hricak H. 2016 New Horizons Lecture: beyond imaging—radiology of tomorrow. *Radiology* 2018;286(3):764–775.
- Lecun Y, Bottou L, Bengio Y, Haffner P. Gradient-based learning applied to document recognition. *Proc IEEE* 1998;86(11):2278–2324.
- Krizhevsky AS, Hinton G. Imagenet classification with deep convolutional neural networks. *Proceedings of the Advances in Neural Information Processing Systems*, 2012; 1097–105.
- Chartrand G, Cheng PM, Vorontsov E, et al. Deep learning: a primer for radiologists. *RadioGraphics* 2017;37(7):2113–2131.
- Litjens G, Kooi T, Bejnordi BE, et al. A survey on deep learning in medical image analysis. *Med Image Anal* 2017;42:60–88.
- Dreyer KJ, Geis JR. When machines think: radiology's next frontier. *Radiology* 2017;285(3):713–718.
- Greenspan H, van Ginneken B, Summers RM. Guest editorial deep learning in medical imaging: Overview and future promise of an exciting new technique. *IEEE Trans Med Imaging* 2016;35(5):1153–1159.
- Erickson BJ, Korfiatis P, Akkuz Z, Kline TL. Machine learning for medical imaging. *RadioGraphics* 2017;37(2):505–515.
- Lee JG, Jun S, Cho YW, et al. Deep learning in medical imaging: general overview. *Korean J Radiol* 2017;18(4):570–584.
- Shen D, Wu G, Suk HI. Deep learning in medical image analysis. *Annu Rev Biomed Eng* 2017;19(1):221–248.
- Ker J, Wang L, Rao J, Lim T. Deep learning applications in medical image analysis. *IEEE Access* 2018;6:9375–9389.
- Suzuki K. Overview of deep learning in medical imaging. *Radiological Phys Technol* 2017;10(3):257–273.
- Klang E. Deep learning and medical imaging. *J Thorac Dis* 2018;10(3):1325–1328.
- LeCun Y, Bengio Y, Hinton G. Deep learning. *Nature* 2015;521(7553):436–444.
- Yosinski J, Clune J, Nguyen A, Fuchs T, Lipson H. Understanding neural networks through deep visualization. *arXiv preprint arXiv:150606579*. 2015. <https://arxiv.org/abs/1506.06579>. Accessed November 21, 2018.
- Lakhani P, Prater AB, Hutson RK, et al. Machine learning in radiology: applications beyond image interpretation. *J Am Coll Radiol* 2018;15(2):350–359. <http://adsabs.harvard.edu/abs/2014arXiv1408.5093J>. Accessed June 1, 2014.
- ImageNet. <http://www.image-net.org/>. Accessed November 21, 2018.
- Hope T, Resheff YS, Lieder I. *Learning TensorFlow: a guide to building deep learning systems*. Sebastopol, Calif: O'Reilly Media, 2017.
- Park SH, Han K. Methodologic guide for evaluating clinical performance and effect of artificial intelligence technology for medical diagnosis and prediction. *Radiology* 2018;286(3):800–809.
- Jia Y, Shelhamer E, Donahue J, et al. Caffe: Convolutional Architecture for Fast Feature Embedding. *ArXiv e-prints [serial online]*. 2014; vol 1408. <http://adsabs.harvard.edu/abs/2014arXiv1408.5093J>. Accessed June 1, 2014.
- Bastien F, Lamblin P, Pascanu R, et al. Theano: new features and speed improvements. *ArXiv e-prints [serial online]*. 2012; vol 1211. <http://adsabs.harvard.edu/abs/2012arXiv1211.5590B>. Accessed November 1, 2012.
- Jia Y, Shelhamer E, Donahue J, et al. Caffe: Convolutional Architecture for Fast Feature Embedding. *ArXiv e-prints [serial online]*. 2014. <https://ui.adsabs.harvard.edu/#abs/2014arXiv1408.5093J>. Accessed June 1, 2014.
- Abadi M, Agarwal A, Barham P, et al. TensorFlow: large-scale machine learning on heterogeneous distributed systems. *ArXiv e-prints [serial online]*. 2016. <https://ui.adsabs.harvard.edu/#abs/2016arXiv160304467A>. Accessed March 1, 2016.
- Collobert R, Kavukcuoglu K, Farabet C. Torch7: A matlab-like environment for machine learning. *BigLearn, NIPS workshop*, 2011.
- Keras. Keras: The Python deep learning library. <https://keras.io/>. Updated June 6, 2018. Accessed November 21, 2018.
- Szegedy C, Liu W, Jia Y, et al. Going deeper with convolutions. *ArXiv e-prints [serial online]*. 2014; vol 1409. <http://adsabs.harvard.edu/abs/2014arXiv1409.4842S>. Accessed September 1, 2014.
- Simonyan K, Zisserman A. Very deep convolutional networks for large-scale image recognition. *ArXiv e-prints [serial online]*. 2014; vol 1409. <http://adsabs.harvard.edu/abs/2014arXiv1409.1556S>. Accessed September 1, 2014.
- Ronneberger O, Fischer P, Brox T. U-Net: convolutional networks for biomedical image segmentation. *ArXiv e-prints [serial online]*. 2015; vol 1505. <http://adsabs.harvard.edu/abs/2015arXiv150504597R>. Accessed May 1, 2015.
- Pang S, Yu Z, Orgun MA. A novel end-to-end classifier using domain transferred deep convolutional neural networks for biomedical images. *Comput Methods Programs Biomed* 2017;140:283–293.
- Bar Y, Diamant I, Wolf L, Lieberman S, Konen E, Greenspan H. Chest pathology detection using deep learning with non-medical training. *Biomedical Imaging (ISBI), 2015 IEEE 12th International Symposium on*. IEEE, 2015; 294–297.
- Refaeilzadeh P, Tang L, Liu H. Cross-validation. In: Liu L, Özsu MT, eds. *Encyclopedia of database systems*. New York, NY: Springer, 2016; 1–7.
- Kohavi R. A study of cross-validation and bootstrap for accuracy estimation and model selection. Montreal, Canada: Ijcai, 1995; 1137–1145.
- Suk HI, Lee SW, Shen D; Alzheimer's Disease Neuroimaging Initiative. Deep ensemble learning of sparse regression models for brain disease diagnosis. *Med Image Anal* 2017;37:101–113.
- Gao XW, Hui R, Tian Z. Classification of CT brain images based on deep learning networks. *Comput Methods Programs Biomed* 2017;138:49–56.
- Li R, Zhang W, Suk HI, et al. Deep learning based imaging data completion for improved brain disease diagnosis. *Med Image Comput Comput Assist Interv* 2014;17(Pt 3):305–312.
- Meszlányi RJ, Buza K, Vidnyánszky Z. Resting state fMRI functional connectivity-based classification using a convolutional neural network architecture. *Front Neuroinform* 2017;11:61.
- Liu M, Zhang J, Adeli E, Shen D. Landmark-based deep multi-instance learning for brain disease diagnosis. *Med Image Anal* 2018;43:157–168.
- Singh S, Srivastava A, Mi L, et al. Deep learning based classification of FDG-PET data for Alzheimers disease categories. *Proc SPIE Int Soc Opt Eng* 2017;10572.
- Zhang J, Liu M, Shen D. Detecting anatomical landmarks from limited medical imaging data using two-stage task-oriented deep neural networks. *IEEE Trans Image Process* 2017;26(10):4753–4764.
- Chen H, Dou Q, Yu L, Qin J, Heng PA. VoxResNet: deep voxelwise residual networks for brain segmentation from 3D MR images. *Neuroimage* 2018;170:446–455.
- Wachinger C, Reuter M, Klein T. DeepNAT: deep convolutional neural network for segmenting neuroanatomy. *Neuroimage* 2018;170:434–445.
- Dolz J, Desrosiers C, Ben Ayed I. 3D fully convolutional networks for subcortical segmentation in MRI: a large-scale study. *Neuroimage* 2018;170:456–470.
- Choi H, Jin KH. Fast and robust segmentation of the striatum using deep convolutional neural networks. *J Neurosci Methods* 2016;274:146–153.
- Mohseni Salehi SS, Erdogmus D, Gholipour A. Auto-context convolutional neural network (Auto-Net) for brain extraction in magnetic resonance imaging. *IEEE Trans Med Imaging* 2017;36(11):2319–2330.
- Mehta R, Majumdar A, Sivaswamy J. BrainSegNet: a convolutional neural network architecture for automated segmentation of human brain structures. *J Med Imaging (Bellingham)* 2017;4(2):024003.
- Moeskops P, Viergever MA, Mendrik AM, de Vries LS, Benders MJ, Išgum I. Automatic segmentation of MR brain images with a convolutional neural network. *IEEE Trans Med Imaging* 2016;35(5):1252–1261.
- Moeskops P, de Bresser J, Kuijff HJ, et al. Evaluation of a deep learning approach for the segmentation of brain tissues and white matter hyperintensities of presumed vascular origin in MRI. *Neuroimage Clin* 2017;17:251–262.
- Kleesiek J, Urban G, Hubert A, et al. Deep MRI brain extraction: a 3D convolutional neural network for skull stripping. *Neuroimage* 2016;129:460–469.
- Choi H, Ha S, Im HJ, Paek SH, Lee DS. Refining diagnosis of Parkinson's disease with deep learning-based interpretation of dopamine transporter imaging. *Neuroimage Clin* 2017;16:586–594.
- Vincent N, Stier N, Yu S, Liebeskind DS, Wang DJ, Scalzo F. Detection of hyperperfusion on arterial spin labeling using deep learning. *Proceedings IEEE Int Conf Bioinformatics Biomed* 2015;2015:1322–1327.
- Zhao X, Wu Y, Song G, Li Z, Zhang Y, Fan Y. A deep learning model integrating FCNNs and CRFs for brain tumor segmentation. *Med Image Anal* 2018;43:98–111.
- Kamnitsas K, Ledig C, Newcombe VFJ, et al. Efficient multi-scale 3D CNN with fully connected CRF for accurate brain lesion segmentation. *Med Image Anal* 2017;36:61–78.
- Liu Y, Stojadinovic S, Hryckushko B, et al. A deep convolutional neural network-based automatic delineation strategy for multiple brain metastases stereotactic radiosurgery. *PLoS One* 2017;12(10):e0185844.
- Korfiatis P, Kline TL, Erickson BJ. Automated segmentation of hyperintense regions in FLAIR MRI using deep learning. *Tomography* 2016;2(4):334–340.
- Li Z, Wang Y, Yu J, et al. Low-grade glioma segmentation based on CNN with fully connected CRF. *J Healthc Eng* 2017;2017:9283480.
- Han X. MR-based synthetic CT generation using a deep convolutional neural network method. *Med Phys* 2017;44(4):1408–1419.
- Stier N, Vincent N, Liebeskind D, Scalzo F. Deep learning of tissue fate features in acute ischemic stroke. *Proceedings IEEE Int Conf Bioinformatics Biomed* 2015;2015:1316–1321.

59. Nakao T, Hanaoka S, Nomura Y, et al. Deep neural network-based computer-assisted detection of cerebral aneurysms in MR angiography. *J Magn Reson Imaging* 2018;47(4):948–953.
60. Ghafoorian M, Karssemeijer N, Heskens T, et al. Deep multi-scale location-aware 3D convolutional neural networks for automated detection of lacunes of presumed vascular origin. *Neuroimage Clin* 2017;14:391–399.
61. Chen L, Bentley P, Rueckert D. Fully automatic acute ischemic lesion segmentation in DWI using convolutional neural networks. *Neuroimage Clin* 2017;15:633–643.
62. Golkov V, Dosovitskiy A, Sperl JI, et al. q-Space deep learning: twelve-fold shorter and model-free diffusion MRI scans. *IEEE Trans Med Imaging* 2016;35(5):1344–1351.
63. Lekadir K, Galimzianova A, Betriu A, et al. A convolutional neural network for automatic characterization of plaque composition in carotid ultrasound. *IEEE J Biomed Health Inform* 2017;21(1):48–55.
64. Qi Dou, Hao Chen, Lequan Yu, et al. Automatic detection of cerebral microbleeds from MR images via 3D convolutional neural networks. *IEEE Trans Med Imaging* 2016;35(5):1182–1195.
65. Chatsias A, Joyce T, Giuffrida MV, Tsafiris SA. Multimodal MR synthesis via modality-invariant latent representation. *IEEE Trans Med Imaging* 2017;37(3):1.
66. Li Z, Wang Y, Yu J, Guo Y, Cao W. Deep learning based radiomics (DLR) and its usage in noninvasive IDH1 prediction for low grade glioma. *Sci Rep* 2017;7(1):5467.
67. Chang K, Bai HX, Zhou H, et al. Residual convolutional neural network for the determination of *IDH* status in low- and high-grade gliomas from MR imaging. *Clin Cancer Res* 2018;24(5):1073–1081.
68. Valverde S, Cabezas M, Roura E, et al. Improving automated multiple sclerosis lesion segmentation with a cascaded 3D convolutional neural network approach. *Neuroimage* 2017;155:159–168.
69. Kim KH, Choi SH, Park SH. Improving arterial spin labeling by using deep learning. *Radiology* 2018;287(2):658–666.
70. Korfiatis P, Kline TL, Lachance DH, Parney IF, Buckner JC, Erickson BJ. Residual deep convolutional neural network predicts MGMT methylation status. *J Digit Imaging* 2017;30(5):622–628.
71. Han L, Kamdar MR. MRI to MGMT: predicting methylation status in glioblastoma patients using convolutional recurrent neural networks. *Pac Symp Biocomput* 2018;23:331–342.
72. Ibragimov B, Xing L. Segmentation of organs-at-risks in head and neck CT images using convolutional neural networks. *Med Phys* 2017;44(2):547–557.
73. Nie D, Zhang H, Adeli E, Liu L, Shen D. 3D deep learning for multi-modal imaging-guided survival time prediction of brain tumor patients. *Med Image Comput Comput Assist Interv* 2016;9901:212–220.
74. Lao J, Chen Y, Li ZC, et al. A deep learning-based radiomics model for prediction of survival in glioblastoma multiforme. *Sci Rep* 2017;7(1):10353.
75. Ma J, Wu F, Jiang T, Zhao Q, Kong D. Ultrasound image-based thyroid nodule automatic segmentation using convolutional neural networks. *Int J CARS* 2017;12(11):1895–1910.
76. Ma J, Wu F, Jiang T, Zhu J, Kong D. Cascade convolutional neural networks for automatic detection of thyroid nodules in ultrasound images. *Med Phys* 2017;44(5):1678–1691.
77. Cole JH, Poudel RPK, Tsagkrasoulis D, et al. Predicting brain age with deep learning from raw imaging data results in a reliable and heritable biomarker. *Neuroimage* 2017;163:115–124.
78. Zhang W, Li R, Deng H, et al. Deep convolutional neural networks for multi-modality iso-intense infant brain image segmentation. *Neuroimage* 2015;108:214–224.
79. Wang SH, Lv YD, Sui Y, Liu S, Wang SJ, Zhang YD. Alcoholism detection by data augmentation and convolutional neural network with stochastic pooling. *J Med Syst* 2017;42(1):2.
80. Chi J, Walia E, Babyn P, Wang J, Groot G, Eramian M. Thyroid nodule classification in ultrasound images by fine-tuning deep convolutional neural network. *J Digit Imaging* 2017;30(4):477–486.
81. Ma J, Wu F, Zhu J, Xu D, Kong D. A pre-trained convolutional neural network based method for thyroid nodule diagnosis. *Ultrasonics* 2017;73:221–230.
82. Larson DB, Chen MC, Lungren MP, Halabi SS, Stence NV, Langlotz CP. Performance of a deep-learning neural network model in assessing skeletal maturity on pediatric hand radiographs. *Radiology* 2018;287(1):313–322.
83. Lee H, Tajmir S, Lee J, et al. Fully automated deep learning system for bone age assessment. *J Digit Imaging* 2017;30(4):427–441.
84. Spampinato C, Palazzo S, Giordano D, Aldinucci M, Leonardi R. Deep learning for automated skeletal bone age assessment in X-ray images. *Med Image Anal* 2017;36:41–51.
85. Kim JR, Shim WH, Yoon HM, et al. Computerized bone age estimation using deep learning based program: evaluation of the accuracy and efficiency. *AJR Am J Roentgenol* 2017;209(6):1374–1380.
86. Jamaludin A, Kadir T, Zisserman A. SpineNet: automated classification and evidence visualization in spinal MRIs. *Med Image Anal* 2017;41:63–73.
87. Prason A, Petersen K, Igel C, Lauze F, Dam E, Nielsen M. Deep feature learning for knee cartilage segmentation using a triplanar convolutional neural network. *Med Image Comput Comput Assist Interv* 2013;16(Pt 2):246–253.
88. Xue Y, Zhang R, Deng Y, Chen K, Jiang T. A preliminary examination of the diagnostic value of deep learning in hip osteoarthritis. *PLoS One* 2017;12(6):e0178992.
89. Cai Y, Landis M, Laidley DT, Kornecki A, Lum A, Li S. Multi-modal vertebrae recognition using transformed deep convolution network. *Comput Med Imaging Graph* 2016;51:11–19.
90. Forsberg D, Sjöblom E, Sunshine JL. Detection and labeling of vertebrae in MR images using deep learning with clinical annotations as training data. *J Digit Imaging* 2017;30(4):406–412.
91. Yang Li, Wei Liang, Yinlong Zhang, Haibo An, Jindong Tan. Automatic lumbar vertebrae detection based on feature fusion deep learning for partial occluded C-arm x-ray images. *Conf Proc IEEE Eng Med Biol Soc* 2016;2016:647–650.
92. Ruhan Sa, Owens W, Wiegand R, et al. Intervertebral disc detection in x-ray images using faster R-CNN. *Conf Proc IEEE Eng Med Biol Soc* 2017;2017:564–567.
93. Hetherington J, Lessoway V, Gunka V, Abolmaesumi P, Rohling R. SLIDE: automatic spine level identification system using a deep convolutional neural network. *Int J CARS* 2017;12(7):1189–1198.
94. Lee H, Troschel FM, Tajmir S, et al. Pixel-level deep segmentation: artificial intelligence quantifies muscle on computed tomography for body morphometric analysis. *J Digit Imaging* 2017;30(4):487–498.
95. Burlina P, Billings S, Joshi N, Albayda J. Automated diagnosis of myositis from muscle ultrasound: exploring the use of machine learning and deep learning methods. *PLoS One* 2017;12(8):e0184059.
96. Wang J, Fang Z, Lang N, Yuan H, Su MY, Baldi P. A multi-resolution approach for spinal metastasis detection using deep Siamese neural networks. *Comput Biol Med* 2017;84:137–146.
97. Wang Y, Qiu Y, Thai T, Moore K, Liu H, Zheng B. A two-step convolutional neural network based computer-aided detection scheme for automatically segmenting adipose tissue volume depicting on CT images. *Comput Methods Programs Biomed* 2017;144:97–104.
98. Banerjee I, Crawley A, Bhethanabotla M, Daldrup-Link HE, Rubin DL. Transfer learning on fused multiparametric MR images for classifying histopathological subtypes of rhabdomyosarcoma. *Comput Med Imaging Graph* 2018;65:167–175.
99. Belharbi S, Chatelain C, Héroult R, et al. Spotting L3 slice in CT scans using deep convolutional network and transfer learning. *Comput Biol Med* 2017;87:95–103.
100. Olczak J, Fahlberg N, Maki A, et al. Artificial intelligence for analyzing orthopedic trauma radiographs. *Acta Orthop* 2017;88(6):581–586.
101. Ciompi F, de Hoop B, van Riel SJ, et al. Automatic classification of pulmonary peri-fissural nodules in computed tomography using an ensemble of 2D views and a convolutional neural network out-of-the-box. *Med Image Anal* 2015;26(1):195–202.
102. Ciompi F, Chung K, van Riel SJ, et al. Towards automatic pulmonary nodule management in lung cancer screening with deep learning. *Sci Rep* 2017;7(1):46479.
103. Song Q, Zhao L, Luo X, Dou X. Using deep learning for classification of lung nodules on computed tomography images. *J Healthc Eng* 2017;2017:8314740.
104. Hua KL, Hsu CH, Hidayati SC, Cheng WH, Chen YJ. Computer-aided classification of lung nodules on computed tomography images via deep learning technique. *Oncotargets Ther* 2015;8:2015–2022.
105. Nibali A, He Z, Wollersheim D. Pulmonary nodule classification with deep residual networks. *Int J CARS* 2017;12(10):1799–1808.
106. Wang H, Zhao T, Li LC, et al. A hybrid CNN feature model for pulmonary nodule malignancy risk differentiation. *JXRays Sci Technol* 2018;26(2):171–187.
107. Sihong Chen, Jing Qin, Xing Ji, et al. Automatic scoring of multiple semantic attributes with multi-task feature leverage: a study on pulmonary nodules in CT images. *IEEE Trans Med Imaging* 2017;36(3):802–814.
108. Tu X, Xie M, Gao J, et al. Automatic categorization and scoring of solid, part-solid and non-solid pulmonary nodules in CT images with convolutional neural network. *Sci Rep* 2017;7(1):8533.
109. Kang G, Liu K, Hou B, Zhang N. 3D multi-view convolutional neural networks for lung nodule classification. *PLoS One* 2017;12(11):e0188290.
110. Sun W, Zheng B, Qian W. Automatic feature learning using multichannel ROI based on deep structured algorithms for computerized lung cancer diagnosis. *Comput Biol Med* 2017;89:530–539.



111. Setio AAA, Traverso A, de Bel T, et al. Validation, comparison, and combination of algorithms for automatic detection of pulmonary nodules in computed tomography images: the LUNA16 challenge. *Med Image Anal* 2017;42:1–13.
112. Teramoto A, Fujita H, Yamamuro O, Tamaki T. Automated detection of pulmonary nodules in PET/CT images: ensemble false-positive reduction using a convolutional neural network technique. *Med Phys* 2016;43(6):2821–2827.
113. Jiang H, Ma H, Qian W, et al. An automatic detection system of lung nodule based on multigroup patch-based deep learning network. *IEEE J Biomed Health Inform* 2018;22(4):1227–1237.
114. Wang C, Elazab A, Wu J, Hu Q. Lung nodule classification using deep feature fusion in chest radiography. *Comput Med Imaging Graph* 2017;57:10–18.
115. Nasr-Esfahani E, Samavi S, Karimi N, et al. Vessel extraction in x-ray angiograms using deep learning. *Conf Proc IEEE Eng Med Biol Soc* 2016;2016:643–646.
116. Yang W, Chen Y, Liu Y, et al. Cascade of multi-scale convolutional neural networks for bone suppression of chest radiographs in gradient domain. *Med Image Anal* 2017;35:421–433.
117. Wang H, Zhou Z, Li Y, et al. Comparison of machine learning methods for classifying mediastinal lymph node metastasis of non-small cell lung cancer from <sup>18</sup>F-FDG PET/CT images. *EJNMMI Res* 2017;7(1):11.
118. Roth HR, Lu L, Seff A, et al. A new 2.5D representation for lymph node detection using random sets of deep convolutional neural network observations. *Med Image Comput Assist Interv* 2014;17(Pt 1):520–527.
119. Wang S, Zhou M, Liu Z, et al. Central focused convolutional neural networks: Developing a data-driven model for lung nodule segmentation. *Med Image Anal* 2017;40:172–183.
120. Umehara K, Ota J, Ishida T. Application of super-resolution convolutional neural network for enhancing image resolution in chest CT. *J Digit Imaging* 2018;31(4):441–450.
121. Anthimopoulos M, Christodoulidis S, Ebner L, Christe A, Mougiakakou S. Lung pattern classification for interstitial lung diseases using a deep convolutional neural network. *IEEE Trans Med Imaging* 2016;35(5):1207–1216.
122. Kim GB, Jung KH, Lee Y, et al. Comparison of shallow and deep learning methods on classifying the regional pattern of diffuse lung disease. *J Digit Imaging* 2018;31(4):415–424.
123. González J, Ash SY, Vegas-Sánchez-Ferrero G, et al. Disease staging and prognosis in smokers using deep learning in chest computed tomography. *Am J Respir Crit Care Med* 2018;197(2):193–203.
124. Wang Q, Zheng Y, Yang G, Jin W, Chen X, Yin Y. Multiscale rotation-invariant convolutional neural networks for lung texture classification. *IEEE J Biomed Health Inform* 2018;22(1):184–195.
125. Christodoulidis S, Anthimopoulos M, Ebner L, Christe A, Mougiakakou S. Multisource transfer learning with convolutional neural networks for lung pattern analysis. *IEEE J Biomed Health Inform* 2017;21(1):76–84.
126. Lee H, Mansouri M, Tajmir S, Lev MH, Do S. A deep-learning system for fully-automated peripherally inserted central catheter (PICC) tip detection. *J Digit Imaging* 2018;31(4):393–402.
127. Fechter T, Adebahr S, Baltas D, Ben Ayed I, Desrosiers C, Dolz J. Esophagus segmentation in CT via 3D fully convolutional neural network and random walk. *Med Phys* 2017;44(12):6341–6352.
128. Zhou X, Takayama R, Wang S, Hara T, Fujita H. Deep learning of the sectional appearances of 3D CT images for anatomical structure segmentation based on an FCN voting method. *Med Phys* 2017;44(10):5221–5233.
129. Lakhani P, Sundaram B. Deep learning at chest radiography: automated classification of pulmonary tuberculosis by using convolutional neural networks. *Radiology* 2017;284(2):574–582.
130. Lopes UK, Valiati JF. Pre-trained convolutional neural networks as feature extractors for tuberculosis detection. *Comput Biol Med* 2017;89:135–143.
131. Oakden-Rayner L, Carneiro G, Bessen T, Nascimento JC, Bradley AP, Palmer LJ. Precision radiology: predicting longevity using feature engineering and deep learning methods in a radiomics framework. *Sci Rep* 2017;7(1):1648.
132. Rajkumar A, Lingam S, Taylor AG, Blum M, Mongan J. High-throughput classification of radiographs using deep convolutional neural networks. *J Digit Imaging* 2017;30(1):95–101.
133. Ypsilantis PP, Siddique M, Sohn HM, et al. Predicting response to neoadjuvant chemotherapy with pet imaging using convolutional neural networks. *PLoS One* 2015;10(9):e0137036.
134. Cicero M, Bilbily A, Colak E, et al. Training and validating a deep convolutional neural network for computer-aided detection and classification of abnormalities on frontal chest radiographs. *Invest Radiol* 2017;52(5):281–287.
135. Abdi AH, Luong C, Tsang T, et al. Automatic quality assessment of echocardiograms using convolutional neural networks: feasibility on the apical four-chamber view. *IEEE Trans Med Imaging* 2017;36(6):1221–1230.
136. Wolterink JM, Leiner T, de Vos BD, van Hamersvelt RW, Viergever MA, Išgum I. Automatic coronary artery calcium scoring in cardiac CT angiography using paired convolutional neural networks. *Med Image Anal* 2016;34:123–136.
137. Dou Q, Yu L, Chen H, et al. 3D deeply supervised network for automated segmentation of volumetric medical images. *Med Image Anal* 2017;41:40–54.
138. Avendi MR, Kheradvar A, Jafarkhani H. A combined deep-learning and deformable-model approach to fully automatic segmentation of the left ventricle in cardiac MRI. *Med Image Anal* 2016;30:108–119.
139. Tan LK, Liew YM, Lim E, McLaughlin RA. Convolutional neural network regression for short-axis left ventricle segmentation in cardiac cine MR sequences. *Med Image Anal* 2017;39:78–86.
140. Yang F, He Y, Hussain M, Xie H, Lei P. Convolutional neural network for the detection of end-diastole and end-systole frames in free-breathing cardiac magnetic resonance imaging. *Comput Math Methods Med* 2017;2017:1640835.
141. Schlemper J, Caballero J, Hajnal JV, Price AN, Rueckert D. A deep cascade of convolutional neural networks for dynamic MR image reconstruction. *IEEE Trans Med Imaging* 2018;37(2):491–503.
142. Zreik M, Lessmann N, van Hamersvelt RW, et al. Deep learning analysis of the myocardium in coronary CT angiography for identification of patients with functionally significant coronary artery stenosis. *Med Image Anal* 2018;44:72–85.
143. Zhen Yu, Dong Ni, Siping Chen, Shengli Li, Tianfu Wang, Baiying Lei. Fetal facial standard plane recognition via very deep convolutional networks. *Conf Proc IEEE Eng Med Biol Soc* 2016;2016:627–630.
144. Yaqub M, Kelly B, Papageorghiou AT, Noble JA. A deep learning solution for automatic fetal neurosonographic diagnostic plane verification using clinical standard constraints. *Ultrasound Med Biol* 2017;43(12):2925–2933.
145. Chen H, Ni D, Qin J, et al. Standard plane localization in fetal ultrasound via domain transferred deep neural networks. *IEEE J Biomed Health Inform* 2015;19(5):1627–1636.
146. Yan L, Rong X, Jun O, Iwata H. Automatic fetal body and amniotic fluid segmentation from fetal ultrasound images by encoder-decoder network with inner layers. *Conf Proc IEEE Eng Med Biol Soc* 2017;2017:1485–1488.
147. Huynh BQ, Li H, Giger ML. Digital mammographic tumor classification using transfer learning from deep convolutional neural networks. *J Med Imaging (Bellingham)* 2016;3(3):034501.
148. Arevalo J, González FA, Ramos-Pollán R, Oliveira JL, Guevara Lopez MA. Representation learning for mammography mass lesion classification with convolutional neural networks. *Comput Methods Programs Biomed* 2016;127:248–257.
149. Kooi T, van Ginneken B, Karssemeijer N, den Heeten A. Discriminating solitary cysts from soft tissue lesions in mammography using a pretrained deep convolutional neural network. *Med Phys* 2017;44(3):1017–1027.
150. Carneiro G, Nascimento J, Bradley AP. Automated analysis of unregistered multi-view mammograms with deep learning. *IEEE Trans Med Imaging* 2017;36(11):2355–2365.
151. Dhungel N, Carneiro G, Bradley AP. A deep learning approach for the analysis of masses in mammograms with minimal user intervention. *Med Image Anal* 2017;37:114–128.
152. Han S, Kang HK, Jeong JY, et al. A deep learning framework for supporting the classification of breast lesions in ultrasound images. *Phys Med Biol* 2017;62(19):7714–7728.
153. Antropova N, Huynh BQ, Giger ML. A deep feature fusion methodology for breast cancer diagnosis demonstrated on three imaging modality datasets. *Med Phys* 2017;44(10):5162–5171.
154. Jadoon MM, Zhang Q, Haq IU, Butt S, Jadoon A. Three-class mammo-gram classification based on descriptive CNN features. *BioMed Res Int* 2017;2017:3640901.
155. Teare P, Fishman M, Benzaquen O, Toledano E, Elnekave E. Malignancy detection on mammography using dual deep convolutional neural networks and genetically discovered false color input enhancement. *J Digit Imaging* 2017;30(4):499–505.
156. Kim DH, Kim ST, Chang JM, Ro YM. Latent feature representation with depth directional long-term recurrent learning for breast masses in digital breast tomosynthesis. *Phys Med Biol* 2017;62(3):1009–1031.
157. Samala RK, Chan HP, Hadjiiski LM, Helvie MA, Cha KH, Richter CD. Multi-task transfer learning deep convolutional neural network: application to computer-aided diagnosis of breast cancer on mammograms. *Phys Med Biol* 2017;62(23):8894–8908.
158. Becker AS, Mueller M, Stoffel E, Marcon M, Ghafoor S, Boss A. Classification of breast cancer in ultrasound imaging using a generic deep learning analysis software: a pilot study. *Br J Radiol* 2018;91(1083):20170576.
159. Becker AS, Marcon M, Ghafoor S, Wurnig MC, Frauenfelder T, Boss A. Deep learning in mammography: diagnostic accuracy of a multipurpose image analysis software in the detection of breast cancer. *Invest Radiol* 2017;52(7):434–440.



160. Kooi T, Karssemeijer N. Classifying symmetrical differences and temporal change for the detection of malignant masses in mammography using deep neural networks. *J Med Imaging (Bellingham)* 2017;4(4):044501.
161. Sun W, Tseng TB, Zhang J, Qian W. Enhancing deep convolutional neural network scheme for breast cancer diagnosis with unlabeled data. *Comput Med Imaging Graph* 2017;57:4–9.
162. Kooi T, Litjens G, van Ginneken B, et al. Large scale deep learning for computer aided detection of mammographic lesions. *Med Image Anal* 2017;35:303–312.
163. Samala RK, Chan HP, Hadjiiski L, Helvie MA, Wei J, Cha K. Mass detection in digital breast tomosynthesis: deep convolutional neural network with transfer learning from mammography. *Med Phys* 2016;43(12):6654–6666.
164. Yap MH, Pons G, Marti J, et al. Automated breast ultrasound lesions detection using convolutional neural networks. *IEEE J Biomed Health Inform* 2018;22(4):1218–1226.
165. Li H, Giger ML, Huynh BQ, Antropova NO. Deep learning in breast cancer risk assessment: evaluation of convolutional neural networks on a clinical dataset of full-field digital mammograms. *J Med Imaging (Bellingham)* 2017;4(4):041304.
166. Wang J, Nishikawa RM, Yang Y. Global detection approach for clustered microcalcifications in mammograms using a deep learning network. *J Med Imaging (Bellingham)* 2017;4(2):024501.
167. Dalmis MU, Litjens G, Holland K, et al. Using deep learning to segment breast and fibroglandular tissue in MRI volumes. *Med Phys* 2017;44(2):533–546.
168. Mohamed AA, Luo Y, Peng H, Jankowitz RC, Wu S. Understanding clinical mammographic breast density assessment: a deep learning perspective. *J Digit Imaging* 2018;31(4):387–392.
169. Mohamed AA, Berg WA, Peng H, Luo Y, Jankowitz RC, Wu S. A deep learning method for classifying mammographic breast density categories. *Med Phys* 2018;45(1):314–321.
170. Li S, Wei J, Chan HP, et al. Computer-aided assessment of breast density: comparison of supervised deep learning and feature-based statistical learning. *Phys Med Biol* 2018;63(2):025005.
171. Wang J, Ding H, Bidgoli FA, et al. Detecting cardiovascular disease from mammograms with deep learning. *IEEE Trans Med Imaging* 2017;36(5):1172–1181.
172. Yasaka K, Akai H. Deep learning with convolutional neural network for differentiation of liver masses at dynamic contrast-enhanced CT: a preliminary study. 2018;286(3):887–96.
173. Vivanti R, Szeskin A, Lev-Cohain N, Sosna J, Joskowicz L. Automatic detection of new tumors and tumor burden evaluation in longitudinal liver CT scan studies. *Int J CARS* 2017;12(11):1945–1957.
174. Hu P, Wu F, Peng J, Bao Y, Chen F, Kong D. Automatic abdominal multi-organ segmentation using deep convolutional neural network and time-implicit level sets. *Int J CARS* 2017;12(3):399–411.
175. Lu F, Wu F, Hu P, Peng Z, Kong D. Automatic 3D liver location and segmentation via convolutional neural network and graph cut. *Int J CARS* 2017;12(2):171–182.
176. Hoogi A, Subramaniam A, Veerapaneni R, Rubin DL. Adaptive estimation of active contour parameters using convolutional neural networks and texture analysis. *IEEE Trans Med Imaging* 2017;36(3):781–791.
177. Mori S. Deep architecture neural network-based real-time image processing for image-guided radiotherapy. *Phys Med* 2017;40:79–87.
178. Ben-Cohen A, Klang E, Diamant I, et al. CT image-based decision support system for categorization of liver metastases into primary cancer sites: initial results. *Acad Radiol* 2017;24(12):1501–1509.
179. Ibragimov B, Toesca D, Chang D, Koong A, Xing L. Combining deep learning with anatomical analysis for segmentation of the portal vein for liver SBRT planning. *Phys Med Biol* 2017;62(23):8943–8958.
180. Esses SJ, Lu X, Zhao T, et al. Automated image quality evaluation of T<sub>2</sub>-weighted liver MRI utilizing deep learning architecture. *J Magn Reson Imaging* 2018;47(3):723–728.
181. Cheng PM, Malhi HS. Transfer learning with convolutional neural networks for classification of abdominal ultrasound images. *J Digit Imaging* 2017;30(2):234–243.
182. Yang X, Liu C, Wang Z, et al. Co-trained convolutional neural networks for automated detection of prostate cancer in multi-parametric MRI. *Med Image Anal* 2017;42:212–227.
183. Cheng R, Roth HR, Lay N, et al. Automatic magnetic resonance prostate segmentation by deep learning with holistically nested networks. *J Med Imaging (Bellingham)* 2017;4(4):041302.
184. Leynes AP, Yang J, Wiesinger F, et al. Zero-echo-time and Dixon deep pseudo-CT (ZeDD CT): direct generation of pseudo-CT images for pelvic PET/MRI attenuation correction using deep convolutional neural networks with multiparametric MRI. *J Nucl Med* 2018;59(5):852–858.
185. Cheng PM, Tejura TK, Tran KN, Whang G. Detection of high-grade small bowel obstruction on conventional radiography with convolutional neural networks. *Abdom Radiol (NY)* 2018;43(5):1120–1127.
186. Liu J, Wang D, Lu L, et al. Detection and diagnosis of colitis on computed tomography using deep convolutional neural networks. *Med Phys* 2017;44(9):4630–4642.
187. Kline TL, Korfiatis P, Edwards ME, et al. Performance of an artificial multi-observer deep neural network for fully automated segmentation of polycystic kidneys. *J Digit Imaging* 2017;30(4):442–448.
188. Liu X, Song JL, Wang SH, Zhao JW, Chen YQ. Learning to diagnose cirrhosis with liver capsule guided ultrasound image classification. *Sensors (Basel)* 2017;17(1):E149.
189. Cha KH, Hadjiiski L, Chan HP, et al. Bladder cancer treatment response assessment in CT using radiomics with deep-learning. *sci rep* 2017;7(1):8738.
190. Cha KH, Hadjiiski L, Samala RK, Chan HP, Caoili EM, Cohan RH. Urinary bladder segmentation in CT urography using deep-learning convolutional neural network and level sets. *Med Phys* 2016;43(4):1882–1896.
191. Cha KH, Hadjiiski LM, Samala RK, et al. Bladder cancer segmentation in CT for treatment response assessment: application of deep-learning convolutional neural network—a pilot study. *Tomography* 2016;2(4):421–429.
192. Wang X, Yang W, Weinreb J, et al. Searching for prostate cancer by fully automated magnetic resonance imaging classification: deep learning versus non-deep learning. *Sci Rep* 2017;7(1):15415.
193. Farag A, Lu L, Roth HR, Liu J, Turkbey E, Summers RM. A bottom-up approach for pancreas segmentation using cascaded superpixels and (deep) image patch labeling. *IEEE Trans Image Process* 2017;26(1):386–399.
194. Yasaka K, Akai H, Kunimatsu A, Abe O, Kiryu S. Liver fibrosis: deep convolutional neural network for staging by using gadoteric acid-enhanced hepatobiliary phase MR images. *Radiology* 2018;287(1):146–155.
195. Trebeschi S, van Griethuysen JJM, Lambregts DMJ, et al. Deep learning for fully-automated localization and segmentation of rectal cancer on multiparametric MR. *Sci Rep* 2017;7(1):5301 [Published correction appears in *Sci Rep* 2018;8(1):2589].
196. Küstner T, Liebgott A, Mauch L, et al. Automated reference-free detection of motion artifacts in magnetic resonance images. *MAGMA* 2018;31(2):243–256.
197. de Vos BD, Wolterink JM, de Jong PA, Leiner T, Viergever MA, Išgum I. ConvNet-based localization of anatomical structures in 3-D medical images. *IEEE Trans Med Imaging* 2017;36(7):1470–1481.
198. Hatt M, Laurent B, Ouhabi A, et al. The first MICCAI challenge on PET tumor segmentation. *Med Image Anal* 2018;44:177–195.
199. Kang E, Min J, Ye JC. A deep convolutional neural network using directional wavelets for low-dose x-ray CT reconstruction. *Med Phys* 2017;44(10):e360–e375.
200. Chen H, Zhang Y, Zhang W, et al. Low-dose CT via convolutional neural network. *Biomed Opt Express* 2017;8(2):679–694.
201. Chen H, Zhang Y, Kalra MK, et al. Low-dose CT with a residual encoder-decoder convolutional neural network. *IEEE Trans Med Imaging* 2017;36(12):2524–2535.
202. Shun Miao, Wang ZJ, Rui Liao. A CNN regression approach for real-time 2D/3D registration. *IEEE Trans Med Imaging* 2016;35(5):1352–1363.
203. Ahmad J, Sajjad M, Mehmood I, Baik SW. SiNC: saliency-injected neural codes for representation and efficient retrieval of medical radiographs. *PLoS One* 2017;12(8):e0181707.
204. Qiu Y, Yan S, Gundreddy RR, et al. A new approach to develop computer-aided diagnosis scheme of breast mass classification using deep learning technology. *J XRay Sci Technol* 2017;25(5):751–763.
205. Liu F, Zhou Z, Jang H, Samsonov A, Zhao G, Kijowski R. Deep convolutional neural network and 3D deformable approach for tissue segmentation in musculoskeletal magnetic resonance imaging. *Magn Reson Med* 2018;79(4):2379–2391.
206. Mayo RC, Leung J. Artificial intelligence and deep learning: radiology's next frontier? *Clin Imaging* 2018;49:87–88.
207. Ebert LC, Heimer J, Schweitzer W, et al. Automatic detection of hemorrhagic pericardial effusion on PMCT using deep learning - a feasibility study. *Forensic Sci Med Pathol* 2017;13(4):426–431.
208. Google Cloud. CLOUD AutoML ALPHA. <https://cloud.google.com/automl/>. Published 2018. Accessed June 14, 2018.
209. Wang X, Peng Y, Lu L, Lu Z, Bagheri M, Summers RM. Chestx-ray8: hospital-scale chest x-ray database and benchmarks on weakly-supervised classification and localization of common thorax diseases. *Computer Vision and Pattern Recognition (CVPR)*, 2017 IEEE Conference on. IEEE, 2017; 3462–3471.
210. Goodfellow IJ, Pouget-Abadie J, Mirza M, et al. Generative adversarial networks. *ArXiv e-prints [serial online]*. 2014; vol 1406. <http://adsabs.harvard.edu/abs/2014arXiv1406.2661G>. Accessed June 1, 2014.